Deciphering the Long-Distance Penguin Contribution to $\bar{B}_{d,s} \to \gamma\gamma$ Decays

Qin Qin,[1,*] Yue-Long Shen,[2,†] Chao Wang,[3,‡] and Yu-Ming Wang[4,§]
[1]*School of Physics, Huazhong University of Science and Technology, Luoyu Road 1037, Wuhan Hubei 430074, People's Republic of China*
[2]*College of Information Science and Engineering, Ocean University of China, Songling Road 238, Qingdao, Shandong 266100, People's Republic of China*
[3]*Department of Mathematics and Physics, Huaiyin Institute of Technology, Meicheng East Road 1, Huaian, Jiangsu 223200, People's Republic of China*
[4]*School of Physics, Nankai University, Weijin Road 94, Tianjin 300071, People's Republic of China*

(Received 11 July 2022; revised 2 October 2022; accepted 9 August 2023; published 31 August 2023)

We compute for the first time the long-distance penguin contribution to the double radiative B-meson decays by applying the perturbative factorization theorem. The numerically dominant penguin amplitude arises from the soft-gluon radiation off the light up-quark loop rather than the counterpart charm-loop effect. Importantly, the long-distance up-quark penguin contribution brings about the substantial cancellation of the known factorizable power correction, thus enabling $B_{d,s} \to \gamma\gamma$ to become new benchmark probes of physics beyond the standard model.

DOI: 10.1103/PhysRevLett.131.091902

Introduction.—It is widely accepted that the exclusive radiative penguin bottom-meson decays play a central role in exploring the quark-flavor dynamics of the standard model (SM) and in probing the nonstandard electroweak interactions at the LHCb and Belle II experiments. In particular, the double radiative $\bar{B}_{d,s} \to \gamma\gamma$ decays with nonhadronic final states offer a remarkably clean environment to address the intricate strong interaction mechanism of the heavy-hadron system with the perturbative factorization technique, in comparison with the radiative decays $\bar{B} \to V\gamma$. Phenomenologically the direct CP asymmetries of the double radiative B-meson decays with the linearly polarized photon states will be also highly beneficial for determining the Cabibbo-Kobayashi-Maskawa phase angle γ [1]. Applying the QCD factorization approach, the leading-power contributions to the exclusive $\bar{B}_{d,s} \to \gamma\gamma$ decay amplitudes in the heavy quark expansion have been demonstrated to be factorized into the short-distance Wilson coefficients and the leading-twist bottom-meson distribution amplitude [2]. In addition, a variety of the subleading-power corrections to $\bar{B}_{d,s} \to \gamma\gamma$ were investigated with the diagrammatic factorization approach [3].

However, the persistent problem of evaluating the long-distance penguin contribution to the double radiative bottom-meson decay amplitudes in the presence of soft-gluon emission remains unresolved at present. For decades the nonlocal subleading power correction arising from the soft-gluon radiation off the charm-loop diagrams has constituted the long-standing obstacle to improve theory computations for the angular observables of $B \to K^{(*)}\ell\ell$ at large hadronic recoil [4–14] (see Refs. [15–17] for discussions on such nonlocal contributions at low recoil). Achieving the robust predictions of the long-distance charm-loop effect in $B \to K^{(*)}\ell\ell$ will be evidently indispensable for disentangling the genuine new physics effect from the SM background contribution and for advancing our understanding toward the nature of the observed flavor anomalies (see for instance Refs. [18–23]). To this end, constructing the systematic formalism to tackle the long-distance penguin contribution to $\bar{B}_{d,s} \to \gamma\gamma$ will further shed new light on the model-independent calculation of the analogous QCD corrections to the flavor-changing neutral current decays $B \to K^{(*)}\ell\bar{\ell}$. More generally, the newly proposed framework to cope with the nonlocal power correction to $\bar{B}_{d,s} \to \gamma\gamma$ will be of importance to perform the precision calculation of the exclusive heavy-flavor baryon decays [24–33].

According to the numerical hierarchy between the bottom and charm quark masses, we will apply the power counting scheme $m_b \gg m_c \sim \mathcal{O}(\sqrt{\Lambda_{\rm QCD} m_b}) \gg \Lambda_{\rm QCD}$ [15,34–37] in establishing the factorization formulas for the long-distance penguin contribution, instead of the alternative counting scheme $m_b \sim m_c \gg \Lambda_{\rm QCD}$ employed in Refs. [38,39]. Subsequently, we will report on a novel observation on the hadronic matrix element responsible for the soft-gluon radiation off the penguin diagrams. Integrating out the short-distance QCD fluctuations embedded in this hadronic quantity will give rise to the generalized three-particle B-meson distribution amplitude in heavy quark effective theory (HQET) defined by the nonlocal matrix element $\langle 0|\bar{q}_s(\tau_1 n)G_{\mu\nu}(\tau_2\bar{n})\Gamma_i h_v(0)|\bar{B}_v\rangle$ rather than the conventional light-cone distribution amplitudes (LCDAs) as previously introduced in Refs. [40,41]. Employing the asymptotic behaviors of this generalized B-meson distribution amplitude determined from the analytic properties of the renormalization-group (RG) evolution equation, we will demonstrate that the soft-collinear convolution integrals entering the factorized expressions of the long-distance penguin contributions converge for both the massless-quark and massive-quark loop induced terms. Phenomenological implications of the newly computed power correction to the double radiative bottom-meson decay observables will be further explored with the three-parameter model for the B-meson soft function.

General analysis.—The effective weak Hamiltonian of the double radiative $b \to q\gamma\gamma$ transitions has been shown to be identical to the one for $b \to q\gamma$ decays [42],

$$\mathcal{H}_{\rm eff} = \frac{4G_F}{\sqrt{2}} \sum_{p=u,c} V_{pb}V_{pq}^* \bigg[C_1(\nu)P_1^{(p)}(\nu) + C_2(\nu)P_2^{(p)}(\nu) + \sum_{i=3}^{8} C_i(\nu)P_i(\nu)\bigg] + \text{H.c.}, \quad (1)$$

by employing the classical equations of motion [43]. We will further adopt the operator basis $P_i^{(p)}$ as advocated in Ref. [44] ensuring the disappearance of Dirac traces involving an odd number of γ_5 in the effective theory computations.

Up to the lowest order in the electromagnetic interaction one can cast the exclusive $\bar{B}_q \to \gamma\gamma$ amplitude in the following form [3]:

$$\bar{\mathcal{A}}(\bar{B}_q \to \gamma\gamma) = -\frac{4G_F}{\sqrt{2}} \frac{\alpha_{\rm em}}{4\pi} \epsilon^{*\alpha}(p)\epsilon^{*\beta}(q) \times \sum_{p=u,c} V_{pb}V_{pq}^* \sum_{i=1}^{8} C_i T_{i,\alpha\beta}^{(p)}, \quad (2)$$

where $T_{i,\alpha\beta}^{(p)}$ can be further decomposed as

$$T_{i,\alpha\beta}^{(p)} = i m_{B_q}^3 \Big[(g_{\alpha\beta}^{\perp} - i\varepsilon_{\alpha\beta}^{\perp})F_{i,L}^{(p)} - (g_{\alpha\beta}^{\perp} + i\varepsilon_{\alpha\beta}^{\perp})F_{i,R}^{(p)}\Big], \quad (3)$$

thanks to the QED Ward-Takahashi identities and the transversality of the on shell photons. Here we have introduced the shorthand notations

$$g_{\alpha\beta}^{\perp} \equiv g_{\alpha\beta} - \frac{n_\alpha \bar{n}_\beta}{2} - \frac{\bar{n}_\alpha n_\beta}{2}, \qquad \varepsilon_{\alpha\beta}^{\perp} \equiv \frac{1}{2}\varepsilon_{\alpha\beta\rho\tau}\bar{n}^\rho n^\tau, \quad (4)$$

by defining two light-cone vectors n_μ and $\bar{n}_\mu$ which satisfy the constraints $p_\mu = m_{B_q}\bar{n}_\mu/2$ and $q_\mu = m_{B_q} n_\mu/2$. It is interesting to note that only the left-handed form factors $F_{i,L}^{(p)}$ will survive at leading order in the heavy quark expansion. Explicitly, the resulting factorization formula for $F_{i,L}^{(p)}$ at leading power can be written as

$$\sum_{i=1}^{8} C_i F_{i,L}^{(p),\rm LP} = -\frac{Q_q f_{B_q} \bar{m}_b(\nu)}{m_{B_q}} V_{7,\rm eff}^{(p)}(m_b,\mu,\nu) \times K^{-1}(m_b,\mu) \int_0^\infty \frac{d\omega}{\omega} \phi_B^+(\omega,\mu) J(m_b,\omega,\mu), \quad (5)$$

where the effective hard function $V_{7,\rm eff}^{(p)}$, the matching coefficient K, and the hard-collinear function J at one loop can be found in Refs. [3,45–47].

QCD factorization for the long-distance penguin contribution.—We are now in a position to explore factorization properties of the subleading power effect from the long-distance penguin contribution by inspecting the partonic diagram in Fig. 1. Both the hard-collinear and the anti-hard-collinear field modes carrying the four-momenta $P_{{\rm hc},\mu} \sim \mathcal{O}(1,\lambda,\lambda^{1/2})$ and $P_{\overline{\rm hc},\mu} \sim \mathcal{O}(\lambda,1,\lambda^{1/2})$ will appear in our problem, where the individual momentum components correspond to $n\cdot P$, $\bar{n}\cdot P$, and $P_\perp$ in sequence for an arbitrary momentum P_μ, and the expansion parameter λ scales as $\Lambda_{\rm QCD}/m_b$. Integrating out the hard-collinear quark loop, one can derive the scattering amplitude of $g(\ell) + b(v) \to q(\tilde{q}) + \gamma(p)$ governed by the effective Hamiltonian [Eq. (1)] by discarding the yet higher-order terms in an expansion of $\Lambda_{\rm QCD}/m_b$ [in comparison with those terms shown in Eq. (6)]

$$\mathcal{M}(g+b\to q+\gamma) = i\frac{4G_F}{\sqrt{2}}\frac{g_{\rm em}g_s}{4\pi^2}\sum_{p=u,c}V_{pb}V_{pq}^*\bigg\{\bigg(C_2-\frac{C_1}{2N_c}\bigg)Q_p[F(z_p)-1] + 6C_6\sum_{q'}Q_{q'}[F(z_{q'})-1] + \bigg[\bigg(C_3-\frac{C_4}{2N_c}\bigg)+16\bigg(C_5-\frac{C_6}{2N_c}\bigg)\bigg]Q_q[F(z_q)-1]\bigg\}\Big[\bar{q}(\tilde{q})\gamma_\beta P_L G_{\mu\alpha}\tilde{F}^{\mu\beta}b(v)\Big]\frac{p^\alpha}{(p-\ell)^2}, \quad (6)$$

where the perturbative penguin function is given by

$$F(x) = 4x\arctan^2\bigg(\frac{1}{\sqrt{4x-1}}\bigg), \quad (7)$$

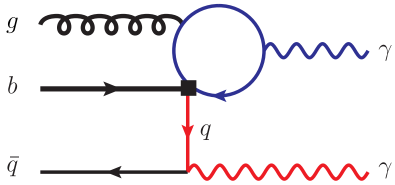

FIG. 1. Diagrammatical representation of the soft-gluon emission from the factorizable quark loop in $\bar{B}_q \to \gamma\gamma$, where the symmetric diagram due to exchanging two on shell photons is not shown. The quark and photon fields marked with red color carry the anti-hard-collinear momenta, while the off shell quark in the fermion loop and the other photon marked with blue color correspond to the hard-collinear fields.

and we have further employed the conventions

$$z_p = \frac{m_p^2 - i0^+}{(p-\ell)^2}, \qquad \tilde{F}^{\mu\nu} = -\left(\frac{1}{2}\right)\epsilon^{\mu\nu\alpha\beta}F_{\alpha\beta}. \tag{8}$$

Importantly, the hard-scattering kernel displayed in Eq. (6) depends on the unique component $\bar{n}\cdot\ell$ of the soft-gluon momentum. Employing the scaling behavior $z_b \sim \mathcal{O}(m_b/\Lambda_{\rm QCD})$, we can verify that the bottom-quark loop diagram with an insertion of P_6 generates the yet higher-order effect compared with the charm-loop effect.

We can proceed to evaluate the amplitude of $g(\ell) + b(v) + \bar{q}(k) \to \gamma(p) + \gamma(q)$ by integrating out the anti-hard-collinear quark propagator in Fig. 1,

$$\begin{aligned}&\langle \gamma(p)\gamma(q)|\bar{q}\gamma_\beta P_L G_{\mu\alpha}\tilde{F}^{\mu\beta} b|g(\ell)b(v)\bar{q}(k)\rangle \\ &\Rightarrow \frac{i g_{\rm em} e_q}{(q-k)^2}\epsilon^{\mu\beta\lambda\tau}p_\lambda \epsilon_\tau^*(p)\epsilon_\rho^*(q)[\bar{q}(k)\gamma_\perp^\rho \not{q}\gamma_\beta P_L G_{\mu\alpha}(\ell)b(v)] \\ &\quad + \mathcal{O}(\alpha_s),\end{aligned} \tag{9}$$

where the short-distance coefficient depends on the component $n\cdot k$ (rather than $\bar{n}\cdot k$) of the soft-quark momentum in the leading-power approximation. We then need to introduce the subleading distribution amplitude defined by the HQET matrix element of $\bar{q}_s(\tau_1 n)G_{\mu\nu}(\tau_2\bar{n})\Gamma_i h_v(0)$. Constructing the general parametrization of this effective matrix element with the covariant tensor formalism [48] (as adopted in Ref. [41]) allows us to derive the factorization formula of the soft-gluon radiative correction to the left-handed helicity form factor

$$\begin{aligned}\sum_{i=1}^{8} C_i F_{i,L}^{(p),\text{soft 4q}} = &-\frac{Q_q f_{B_q}}{m_{B_q}}\int_{-\infty}^{+\infty}\frac{d\omega_1}{\omega_1 - i0}\int_{-\infty}^{+\infty}\frac{d\omega_2}{\omega_2 - i0}\left\{\left(C_2 - \frac{C_1}{2N_c}\right)Q_p[F(z_p)-1] + 6C_6 Q_c[F(z_c)-1]\right. \\ &\left. - \left[\left(C_3 - \frac{C_4}{2N_c}\right) + 16\left(C_5 - \frac{C_6}{2N_c}\right)\right]Q_q\right\}\Phi_{\rm G}(\omega_1,\omega_2,\mu) + \mathcal{O}(\alpha_s).\end{aligned} \tag{10}$$

It is customary to define $\omega_1 = n\cdot k$ and $\omega_2 = \bar{n}\cdot\ell$ such that the resulting hard-collinear function develops a peculiar dependence on ω_2 via the quantity $z_p = -m_p^2/(m_B\omega_2)$ (apart from an overall factor $1/\omega_2$). In accordance with the power-counting rules for the short-distance matching coefficients and the nonperturbative HQET function in the obtained factorization formulas [Eqs. (5) and (10)], we can verify the scaling behavior of the long-distance penguin contribution in the heavy quark expansion

$$\left[\sum_{i=1}^{8} C_i F_{i,L}^{(p),\text{soft 4q}}\right] : \left[\sum_{i=1}^{8} C_i F_{i,L}^{(p),\rm LP}\right] \sim \Lambda_{\rm QCD} : m_{B_q}. \tag{11}$$

Including the higher-order QCD corrections will generate the nontrivial hard functions from matching the effective four-quark operators $P_i^{(p)}$ onto soft-collinear effective theory I (SCET$_{\rm I}$) and simultaneously result in the interesting impacts on the (anti)-hard-collinear matching coefficients that appeared in Eq. (10). Schematically, the factorized expression for the long-distance penguin correction to $\bar{B}_q \to \gamma\gamma$ can be cast in the form $\mathcal{HJ}\star\bar{\mathcal{J}}\star\Phi_{\rm G}$, which resembles the very pattern for the $Q_1^q - Q_{7\gamma}$ contribution to $\bar{B}\to X_s\gamma$ [49] (see also Refs. [50,51]). Moreover, the crossing Feynman diagram due to exchanging the two on shell photons gives rise to the contribution identical to the direct diagram.

The subleading distribution amplitude (more appropriately called *soft function*) $\Phi_{\rm G}$ in Eq. (10) is defined by the matrix element of the nonlocal operator with quark-gluon fields localized on distinct light-cone directions

$$\begin{aligned}&\langle 0|(\bar{q}_s S_n)(\tau_1 n)(S_n^\dagger S_{\bar{n}})(0)(S_{\bar{n}}^\dagger g_s G_{\mu\nu} S_{\bar{n}})(\tau_2\bar{n})\bar{n}^\nu \not{n}\gamma_\perp^\mu\gamma_5(S_{\bar{n}}^\dagger h_v)(0)|\bar{B}_v\rangle \\ &\quad = 2\tilde{f}_B(\mu)m_B\int_{-\infty}^{+\infty}d\omega_1\int_{-\infty}^{+\infty}d\omega_2\exp[-i(\omega_1\tau_1 + \omega_2\tau_2)]\Phi_{\rm G}(\omega_1,\omega_2,\mu),\end{aligned} \tag{12}$$

where the two soft Wilson lines S_n and $S_{\bar{n}}$ (see Ref. [3] for the explicit definitions) are essential to maintain gauge invariance. Comparing with the subleading shape function g_{17} for the inclusive B-meson decays, the distinctive features of $\Phi_{\rm G}$ consist of the nonforward composite operator in the defining matrix element and the appearance of the QCD quark field whose interactions with soft gluons cannot be described by the Eikonal effective theory. Neglecting renormalization effects, the nonlocal HQET matrix element on the left-hand side of Eq. (12) can be described by the familiar three-particle LCDAs when taking the limit $\tau_{1(2)} \to 0$. In contrast to the HQET distribution amplitudes $\Phi_{4,5}$, taking into account the ultraviolet renormalization of $\Phi_{\rm G}$ results in the intriguing pattern of mixing positive into negative support [see Eqs. (7) and (8) of the Supplemental Material [52] for the manifest expression of the evolution equation], thus demanding the different limits of the corresponding convolution integrals in the tree-level normalization conditions

$$\int_{-\infty}^{+\infty} d\omega_1 \Phi_{\rm G}(\omega_1,\omega_2,\mu) = \int_0^{\infty} d\omega_1 \Phi_4(\omega_1,\omega_2,\mu),$$
$$\int_{-\infty}^{+\infty} d\omega_2 \Phi_{\rm G}(\omega_1,\omega_2,\mu) = \int_0^{\infty} d\omega_2 \Phi_5(\omega_1,\omega_2,\mu),$$
$$\int_{-\infty}^{+\infty} d\omega_1 \int_{-\infty}^{+\infty} d\omega_2 \Phi_{\rm G}(\omega_1,\omega_2,\mu) = \frac{\lambda_E^2+\lambda_H^2}{3}, \tag{13}$$

where the explicit definitions of $\Phi_{4,5}$ can be found in Ref. [41]. λ_E^2 and λ_H^2 can be defined by the effective matrix elements of the local chromoelectric and chromomagnetic operators [53]. As already mentioned, the support region of $\Phi_{\rm G}(\omega_1,\omega_2,\mu)$ must be extended to the entire real axes $-\infty < \omega_{1,2} < +\infty$ due to the RG evolution, in analogy to the earlier observation for the QED-generalized soft function of the charmless two-body $\bar{B} \to M_1 M_2$ decays [54]. This distinctive feature for the bottom-meson soft function $\Phi_{\rm G}$ will be maintained even if we initially assume $\omega_1' > 0$ and $\omega_2' > 0$. In particular, the emerged imaginary part in the anomalous dimension $\Gamma(\omega_1,\omega_2,\omega_1',\omega_2')$ implies that the soft function $\Phi_{\rm G}$ for the theory description of the long-distance penguin contributions to $\bar{B}_q \to \gamma\gamma$ becomes complex due to the soft-parton rescattering. Furthermore, the asymptotic behaviors of the RG-evolved soft function can be determined from the analytic properties of the one-loop evolution equation. On the basis of the scaling behaviors for $\Phi_{\rm G}(\omega_1,\omega_2,\mu)$ at $\omega_{1,2} \to 0$ and $\omega_{1,2} \to \pm\infty$ as derived in the Supplemental Material [52] (with the inclusion of Refs. [54–60]), we can verify that the convolution integrals in the factorized expression [Eq. (10)] converge.

As already discussed in Ref. [61], the normalization integrals of the renormalized B-meson LCDAs are divergent due to the singularities of the corresponding position-space amplitudes in the small light-cone separation limit [62]. Analogously, the asymptotic behavior of $\Phi_{\rm G}(\omega_1,\omega_2,\mu)$ at large values of $\omega_{1,2}$ displayed in Eq. (30) of the Supplemental Material [52] indicates that all nonnegative moments of $\Phi_{\rm G}$ diverge. Consequently, the obtained constraints in Eq. (13) do not hold beyond the tree-level approximation. Instead, the model-independent constraints on $\Phi_{\rm G}(\omega_1,\omega_2,\mu)$ at $|\omega_{1,2}| \gg \Lambda_{\rm QCD}$ can be derived from the operator-product-expansion (OPE) analysis of the regularized moments (for $N_{1,2} \geq 0$),

$$M_{N_1,N_2}\left(\Lambda_{\rm UV}^{(1)},\Lambda_{\rm UV}^{(2)},\tilde{\Lambda}_{\rm UV}^{(1)},\tilde{\Lambda}_{\rm UV}^{(2)},\mu\right) = \int_{-\tilde{\Lambda}_{\rm UV}^{(1)}}^{+\Lambda_{\rm UV}^{(1)}} d\omega_1\, \omega_1^{N_1} \int_{-\tilde{\Lambda}_{\rm UV}^{(2)}}^{+\Lambda_{\rm UV}^{(2)}} d\omega_2\, \omega_2^{N_2} \Phi_{\rm G}(\omega_1,\omega_2,\mu), \tag{14}$$

following the Lee-Neubert strategy [61]. One can then construct the improved model for the soft function by gluing continuously the radiative tail $\Phi_{\rm G}^{\rm asy}$ onto the given model function $\Phi_{\rm G}^{\rm mod}$ and by enforcing the OPE constraints on the cut-off moments [61] (see also Refs. [63,64]). We will leave the detailed discussions on the systematic parametrization of $\Phi_{\rm G}$ satisfying the nontrivial short-distance constraints for our future work.

It remains interesting to explore the nonperturbative behavior of the initial condition for $\Phi_{\rm G}$ with the dispersion technique as adopted in Refs. [53,62,65–67]. Starting with the HQET correlation function

$$\Pi_{\rm G} = i \int d^4x \, \exp(-i\omega v\cdot x) \langle 0|{\rm T}\{[(\bar{q}_s S_n)(\tau_1 n) (S_n^\dagger S_{\bar{n}})(0)(S_{\bar{n}}^\dagger g_s G_{\mu\nu} S_{\bar{n}})(\tau_2 \bar{n})\bar{n}^\nu \not{n} \gamma_\perp^\mu \gamma_5 (S_{\bar{n}}^\dagger h_v)(0)], [\bar{h}_v(x) g_s G_{\rho\lambda}(x)\sigma^{\rho\lambda}\gamma_5 q_s(x)]\}|0\rangle, \tag{15}$$

we can on the one hand compute this quantity in the kinematic region $|\omega| \gg \Lambda_{\rm QCD}$ with the OPE technique and on the other hand derive the hadronic representation of $\Pi_{\rm G}$ by taking advantage of analyticity with respect to the variable ω. Matching the above two dispersion representations with the aid of the parton-hadron duality ansätz enables us to extract the scaling behavior $\Phi_{\rm G}(\omega_1,\omega_2,\mu_0) \sim \omega_1\omega_2^2$ at $\omega_{1,2} \to 0$.

Additionally, the theory framework of evaluating the long-distance penguin contribution developed here can be extended to explore the exclusive electroweak penguin decays $B \to K^{(*)}\ell\bar{\ell}$ systematically by investigating the appropriate QCD correlation function with a variety of the subleading soft functions in analogy to $\Phi_{\rm G}$.

Numerical implications.—We turn to address the phenomenological implications of the long-distance penguin contributions to $\bar{B}_q \to \gamma\gamma$ decay amplitudes. To achieve this goal, we will adopt the particular nonperturbative model

$$\Phi_{\rm G}(\omega_1,\omega_2,\mu_0) = \frac{\lambda_E^2+\lambda_H^2}{6}\frac{\omega_1\omega_2^2}{\omega_0^5}\exp\left(-\frac{\omega_1+\omega_2}{\omega_0}\right) \frac{\Gamma(\beta+2)}{\Gamma(\alpha+2)} U\left(\beta-\alpha, 4-\alpha, \frac{\omega_1+\omega_2}{\omega_0}\right) \times \theta(\omega_1)\theta(\omega_2), \tag{16}$$

at $\mu_0 = 1.0$ GeV, motivated from the three-parameter ansätz for the twist-two LCDA [68]. It needs to be stressed that the initial condition of the soft function is assumed to be real and normalizable here. While this ansätz is acceptable for the subsequent numerical analysis, it does not hold strictly due to the presence of the radiative tail and imaginary part at an arbitrary scale. The shape parameters ω_0, α, and β can be determined by enforcing the first and second normalization relations in Eq. (13) and by employing the concrete model of $\Phi_{4,5}$ in Ref. [37]. The leading-logarithmic evolution of Φ_G to the factorization scale μ will be accomplished with the aid of Eq. (21) in the Supplemental Material [52]. The conventional HQET LCDAs in the factorization formulas of $F^{(p)}_{i,L(R)}$ from Ref. [3] will be also in demand, and we will apply the same phenomenological model as presented in this reference, with the exceptions of updated intervals for $\lambda_{B_d} = (275 \pm 75)$ MeV and $\lambda_{B_s} = (325 \pm 75)$ MeV [69] (see Ref. [67] for a recent determination). The allowed intervals of additional input parameters are identical to the ones collected in Ref. [3].

Inspecting the numerical features of the soft-gluon radiative corrections to the helicity form factors displayed in Fig. 1 of the Supplemental Material [52] (with the inclusion of Refs. [3,70–73]) indicates that the newly computed up-quark penguin contribution generates the substantial cancellation of the combined factorizable power corrections discussed in Ref. [3], and the long-distance charm-quark penguin mechanism merely brings about the minor impact on $\sum_i C_i F^{(c)}_{i,L}$. Having at our disposal the desired theory predictions for the helicity form factors, we proceed to explore the phenomenological implications of the long-distance penguin contributions on the CP-averaged branching fractions, the polarization fractions, and the time-dependent CP asymmetries of $\bar{B}_q \to \gamma\gamma$. To achieve this goal, we display our numerical predictions for these interesting observables with three distinct scenarios: (I) including only the leading power contributions at the next-to-leading-logarithmic accuracy, (II) combining the available leading-power contributions with the subleading-power corrections as previously determined in Ref. [3], and (III) adding further the newly determined long-distance penguin contributions.

It is evident from Fig. 2 that the improved predictions for the CP-averaged branching fractions with the inclusion of the long-distance penguin contributions turn out to be only marginally different from the counterpart theory determinations obtained in our previous work [3]. We further present the comparative predictions for the CP-averaged polarization fractions and the CP-violating observables in Figs. 2 and 3 of the Supplemental Material [52], where the explicit definitions of these experimental observables for the double radiative $\bar{B}_q \to \gamma\gamma$ decays in the presence of the neutral-meson mixing are also provided. Interestingly, the power suppressed soft-gluon radiative effects can result in the noticeable impacts on the two particular CP-violating observables $\mathcal{A}_{CP}^{\mathrm{mix},\parallel}$ and $\mathcal{A}_{CP}^{\mathrm{mix},\perp}$: numerically $\mathcal{O}(30\%)$ corrections for both $b \to d\gamma$ and $b \to s\gamma$ transitions with the default inputs. Since the yielding numerical results for the CP-violating observables are generally insensitive to λ_{B_q},

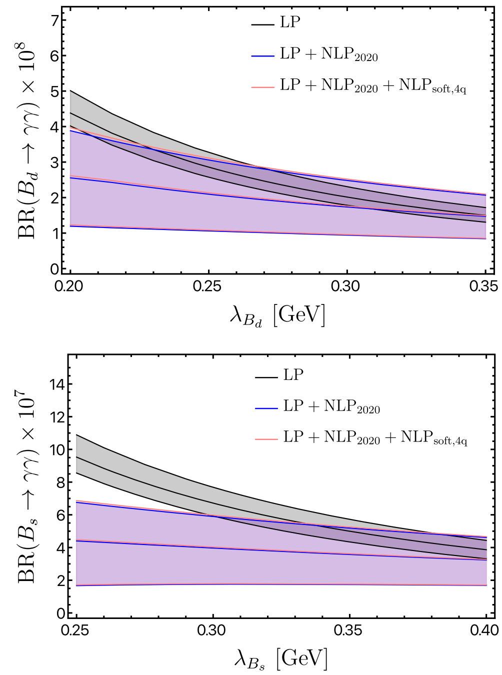

FIG. 2. Theory predictions for the CP-averaged branching fractions of $\bar{B}_d \to \gamma\gamma$ [top] and $\bar{B}_s \to \gamma\gamma$ [down] obtained from including only the leading-power contributions [gray bands], from taking into account both the leading-power contributions and the various subleading-power corrections estimated in Ref. [3] [blue bands], and from adding further the newly determined long-distance penguin corrections [red bands].

we collect here only our predictions of these asymmetries $\{\mathcal{A}_{CP}^{\mathrm{dir},\parallel}, \mathcal{A}_{CP}^{\mathrm{mix},\parallel}, \mathcal{A}_{CP}^{\mathrm{dir},\perp}, \mathcal{A}_{CP}^{\mathrm{mix},\perp}\} = \{13^{+4}_{-3}\%, -19^{+5}_{-8}\%, 34^{+7}_{-5}\%, 13^{+7}_{-6}\%\}$ for $\bar{B}_d \to \gamma\gamma$ at $\lambda_{B_d} = 275$ MeV and $\{\mathcal{A}_{CP}^{\mathrm{dir},\parallel}, \mathcal{A}_{CP}^{\mathrm{mix},\parallel}, \mathcal{A}_{CP}^{\mathrm{dir},\perp}, \mathcal{A}_{CP}^{\mathrm{mix},\perp}\} = \{-0.67^{+0.15}_{-0.23}\%, 0.97^{+0.44}_{-0.27}\%, -1.8^{+0.3}_{-0.5}\%, -0.52^{+0.32}_{-0.41}\%\}$ for $\bar{B}_s \to \gamma\gamma$ at $\lambda_{B_s} = 325$ MeV.

Conclusions.—In conclusion, we have presented the first computation of the long-distance penguin contribution to the double radiative B-meson decays. Adopting the power counting scheme $m_c \sim \mathcal{O}(\sqrt{\Lambda_{\mathrm{QCD}} m_b})$, we demonstrated that the soft function Φ_G defined by the three-body HQET operator with partonic fields localized on two distinct light-ray directions emerged naturally in the factorization formula [Eq. (10)]. Phenomenologically the soft-gluon radiative off the factorizable up-quark loop appeared to bring about a more pronounced effect in comparison with the corresponding charm-quark penguin mechanism. Despite the negligible impacts on the CP-averaged branching fractions, including the long-distance penguin contributions can generate noticeable corrections to our theory predictions for the CP-violating observables $\mathcal{A}_{CP}^{\mathrm{mix},\parallel}$ and $\mathcal{A}_{CP}^{\mathrm{mix},\perp}$. In addition, our analysis will be evidently beneficial for exploring the charming penguin dynamics in $B \to K^*\gamma$ and $B \to K^{(*)}\ell\bar{\ell}$, which are generally recognized as the flagship probes of physics beyond the SM.

The research of Q. Q. is supported by the National Natural Science Foundation of China with Grant No. 12005068. C. W. is supported in part by the National Natural Science Foundation of China with Grant No. 12105112 and the Natural Science Foundation of Jiangsu Education Committee with Grant No. 21KJB140027. The research of Y. L. S. is supported by the National Natural Science Foundation of China with Grant No. 12175218 and the Natural Science Foundation of Shandong with Grant No. ZR2020MA093. Y. M. W. acknowledges support from the National Natural Science Foundation of China with Grants No. 11735010 and No. 12075125, and the Natural Science Foundation of Tianjin with Grant No. 19JCJQJC61100.

*qqin@hust.edu.cn
†Corresponding author: shenylmeteor@ouc.edu.cn
‡Corresponding author: chaowang@nankai.edu.cn
§Corresponding author: wangyuming@nankai.edu.cn

[1] S. W. Bosch and G. Buchalla, J. High Energy Phys. 08 (2002) 054.
[2] S. Descotes-Genon and C. T. Sachrajda, Phys. Lett. B **557**, 213 (2003).
[3] Y.-L. Shen, Y.-M. Wang, and Y.-B. Wei, J. High Energy Phys. 12 (2020) 169.
[4] A. Ali, T. Mannel, and T. Morozumi, Phys. Lett. B **273**, 505 (1991).
[5] A. Khodjamirian, T. Mannel, A. A. Pivovarov, and Y. M. Wang, J. High Energy Phys. 09 (2010) 089.
[6] A. Khodjamirian, T. Mannel, and Y. M. Wang, J. High Energy Phys. 02 (2013) 010.
[7] C. Hambrock, A. Khodjamirian, and A. Rusov, Phys. Rev. D **92**, 074020 (2015).
[8] C. Bobeth, M. Chrzaszcz, D. van Dyk, and J. Virto, Eur. Phys. J. C **78**, 451 (2018).
[9] A. Kozachuk and D. Melikhov, Phys. Lett. B **786**, 378 (2018).
[10] D. Melikhov, EPJ Web Conf. **222**, 01007 (2019).
[11] N. Gubernari, D. van Dyk, and J. Virto, J. High Energy Phys. 02 (2021) 088.
[12] V. G. Chobanova, T. Hurth, F. Mahmoudi, D. Martinez Santos, and S. Neshatpour, J. High Energy Phys. 07 (2017) 025.
[13] A. Arbey, T. Hurth, F. Mahmoudi, and S. Neshatpour, Phys. Rev. D **98**, 095027 (2018).
[14] T. Hurth, F. Mahmoudi, and S. Neshatpour, Phys. Rev. D **102**, 055001 (2020).
[15] B. Grinstein and D. Pirjol, Phys. Rev. D **70**, 114005 (2004).
[16] M. Beylich, G. Buchalla, and T. Feldmann, Eur. Phys. J. C **71**, 1635 (2011).
[17] J. Lyon and R. Zwicky (2014).
[18] S. Jäger and J. Martin Camalich, J. High Energy Phys. 05 (2013) 043.
[19] S. Descotes-Genon, J. Matias, and J. Virto, Phys. Rev. D **88**, 074002 (2013).
[20] S. Descotes-Genon, L. Hofer, J. Matias, and J. Virto, J. High Energy Phys. 06 (2016) 092.
[21] M. Ciuchini, M. Fedele, E. Franco, S. Mishima, A. Paul, L. Silvestrini, and M. Valli, J. High Energy Phys. 06 (2016) 116.
[22] J. Aebischer, W. Altmannshofer, D. Guadagnoli, M. Reboud, P. Stangl, and D. M. Straub, Eur. Phys. J. C **80**, 252 (2020).
[23] M. Ciuchini, M. Fedele, E. Franco, A. Paul, L. Silvestrini, and M. Valli, Phys. Rev. D **103**, 015030 (2021).
[24] C.-H. Chen and C. Q. Geng, Phys. Rev. D **64**, 074001 (2001).
[25] X.-G. He, T. Li, X.-Q. Li, and Y.-M. Wang, Phys. Rev. D **74**, 034026 (2006).
[26] Y.-M. Wang, Y. Li, and C.-D. Lu, Eur. Phys. J. C **59**, 861 (2009).
[27] P. Ball, V. M. Braun, and E. Gardi, Phys. Lett. B **665**, 197 (2008).
[28] Y.-M. Wang, Y.-L. Shen, and C.-D. Lu, Phys. Rev. D **80**, 074012 (2009).
[29] T. Mannel and Y.-M. Wang, J. High Energy Phys. 12 (2011) 067.
[30] T. Feldmann and M. W. Y. Yip, Phys. Rev. D **85**, 014035 (2012); **86**, 079901(E) (2012).
[31] W. Wang, Phys. Lett. B **708**, 119 (2012).
[32] V. M. Braun, S. E. Derkachov, and A. N. Manashov, Phys. Lett. B **738**, 334 (2014).
[33] Y.-M. Wang and Y.-L. Shen, J. High Energy Phys. 02 (2016) 179.
[34] H. Boos, T. Feldmann, T. Mannel, and B. D. Pecjak, Phys. Rev. D **73**, 036003 (2006).
[35] H. Boos, T. Feldmann, T. Mannel, and B. D. Pecjak, J. High Energy Phys. 05 (2006) 056.
[36] Y.-M. Wang, Y.-B. Wei, Y.-L. Shen, and C.-D. Lü, J. High Energy Phys. 06 (2017) 062.
[37] J. Gao, T. Huber, Y. Ji, C. Wang, Y.-M. Wang, and Y.-B. Wei, J. High Energy Phys. 05 (2022) 024.
[38] M. Beneke, G. Buchalla, M. Neubert, and C. T. Sachrajda, Nucl. Phys. **B591**, 313 (2000).
[39] T. Huber, S. Kränkl, and X.-Q. Li, J. High Energy Phys. 09 (2016) 112.
[40] H. Kawamura, J. Kodaira, C.-F. Qiao, and K. Tanaka, Phys. Lett. B **523**, 111 (2001); **536**, 344(E) (2002).
[41] V. M. Braun, Y. Ji, and A. N. Manashov, J. High Energy Phys. 05 (2017) 022.
[42] B. Grinstein, R. P. Springer, and M. B. Wise, Nucl. Phys. **B339**, 269 (1990).
[43] H. D. Politzer, Nucl. Phys. **B172**, 349 (1980).
[44] K. G. Chetyrkin, M. Misiak, and M. Munz, Phys. Lett. B **400**, 206 (1997); **425**, 414(E) (1998).
[45] E. Eichten and B. R. Hill, Phys. Lett. B **234**, 511 (1990).
[46] E. Lunghi, D. Pirjol, and D. Wyler, Nucl. Phys. **B649**, 349 (2003).
[47] S. W. Bosch, R. J. Hill, B. O. Lange, and M. Neubert, Phys. Rev. D **67**, 094014 (2003).
[48] A. F. Falk, H. Georgi, B. Grinstein, and M. B. Wise, Nucl. Phys. **B343**, 1 (1990).
[49] M. Benzke, S. J. Lee, M. Neubert, and G. Paz, J. High Energy Phys. 08 (2010) 099.
[50] T. Hurth and M. Nakao, Annu. Rev. Nucl. Part. Sci. **60**, 645 (2010).
[51] M. Benzke, T. Hurth, and S. Turczyk, J. High Energy Phys. 10 (2017) 031.
[52] See Supplemental Material at http://link.aps.org/supplemental/10.1103/PhysRevLett.131.091902 for the detailed numerical predictions for the helicity form factors and the comprehensive

explorations of renormalization-group properties for the generalized bottom-meson soft function.
[53] A. G. Grozin and M. Neubert, Phys. Rev. D **55**, 272 (1997).
[54] M. Beneke, P. Böer, J.-N. Toelstede, and K. K. Vos, J. High Energy Phys. 08 (2022) 020.
[55] M. Beneke, C. Bobeth, and R. Szafron, J. High Energy Phys. 10 (2019) 232; 11 (2022) 099(E).
[56] M. Beneke, P. Böer, J.-N. Toelstede, and K. K. Vos, J. High Energy Phys. 11 (2020) 081.
[57] B. O. Lange and M. Neubert, Phys. Rev. Lett. **91**, 102001 (2003).
[58] Y.-K. Huang, Y.-L. Shen, C. Wang, Y.-M. Wang, and X.-C. Zhao (to be published).
[59] S. Actis, M. Beneke, P. Falgari, and C. Schwinn, Nucl. Phys. **B807**, 1 (2009).
[60] A. J. Buras, M. Jamin, M. E. Lautenbacher, and P. H. Weisz, Nucl. Phys. **B370**, 69 (1992); **B375**, 501(A) (1992).
[61] S. J. Lee and M. Neubert, Phys. Rev. D **72**, 094028 (2005).
[62] V. M. Braun, D. Y. Ivanov, and G. P. Korchemsky, Phys. Rev. D **69**, 034014 (2004).
[63] T. Feldmann, B. O. Lange, and Y.-M. Wang, Phys. Rev. D **89**, 114001 (2014).
[64] M. Beneke, G. Finauri, K. K. Vos, and Y. Wei, arXiv:2305.06401.
[65] A. Khodjamirian, T. Mannel, and N. Offen, Phys. Rev. D **75**, 054013 (2007).
[66] C.-D. Lü, Y.-L. Shen, Y.-M. Wang, and Y.-B. Wei, J. High Energy Phys. 01 (2019) 024.
[67] A. Khodjamirian, R. Mandal, and T. Mannel, J. High Energy Phys. 10 (2020) 043.
[68] M. Beneke, V. M. Braun, Y. Ji, and Y.-B. Wei, J. High Energy Phys. 07 (2018) 154.
[69] M. Beneke, C. Bobeth, and R. Szafron, Phys. Rev. Lett. **120**, 011801 (2018).
[70] A. Cerri *et al.*, CERN Yellow Rep. Monogr. **7**, 867 (2019).
[71] M. Ciuchini, M. Fedele, E. Franco, A. Paul, L. Silvestrini, and M. Valli, Eur. Phys. J. C **83**, 64 (2023).
[72] W. Altmannshofer and F. Archilli, in 2022 Snowmass Summer Study (2022), arXiv:2206.11331.
[73] W. Altmannshofer *et al.* (Belle-II Collaboration), Prog. Theor. Exp. Phys. **2019**, 123C01 (2019); **2020**, 029201(E) (2020).